Ninth International Conference on CFD in the Minerals and Process Industries
CSIRO, Melbourne, Australia
10-12 December 2012

FLOQUET STABILTY OF TIME PERIODIC PIPE FLOW

Jonathan R. A. NEBAUER[1*] and Hugh M. BLACKBURN[1]

[1] Department of Mechanical and Aerospace Engineering, Monash University, Victoria 3800, AUSTRALIA
*Corresponding author, E-mail address: jonathan.nebauer@monash.edu

ABSTRACT

A Chebyshev spectral co-location and divergence-free method is adapted to solve the linearised Navier-Stokes (LNS) equations for time-periodic pipe flow. The method is spectral in the pipe axis and azimuth, allowing for specific axial and azimuthal wave numbers. A Krylov subspace method is used to find the leading (real-part) eigenvalues of the LNS flow evolution over one oscillation period. We demonstrate the relevance to Floquet Theory and proceed to assess the linear-stability of these flows. The outcomes are compared against known linear stability results in pipe flows. Finally, an apparent discontinuity in the eigenproblem is investigated and explained by its physical and numerical relevance. This investigation lays the ground-work for a validation study of recently presented three-dimensional linear instabilities in periodic pipe flow.

NOMENCLATURE

$\mathcal{A}$	state-transition operator
D	pipe diameter
j	eigenvalue stack, j=1,2,3…
J_0	Bessel function of the zeroth-order
K_n	complex pressure gradient
L	linear differential operator
n	frequency harmonic
p	pressure
r	radial location
R	pipe radius
t	time
T	period
u	primitives velocity (u,v,w)
u'	perturbation velocity
v	solenoidal velocity
W	Solenoidal space
z	axial coordinate
α	axial wave number
β	azimuthal wave number
θ	azimuthal coordinate
ρ	density
ν	kinematic viscosity
ω	circular frequency
μ	Floquet multiplier
Π_0	real pressure gradient

INTRODUCTION

The investigation of time-periodic pipe flows has received renewed interest in the past decade. This may be attributed to an increase in computational power, advances in spectral methodology (to which the geometry is idealised), and the discovery of new autonomous processes in shear flow (Enez and Pinelli, 1999). Industrially, these types of flows and their transitional properties are of critical interest in cardio-related surgery where artificial components are the largest contributor to blood degradation. Peristaltic pumping of delicate suspensions and non-Newtonian fluids are also of importance, where high shear rates can cause damage to both the fluids and the pumping equipment.

It is believed that steady laminar flow in pipes is stable to infinitesimal perturbations (Schmidt and Henningson, 2000), while channels are asymptotically unstable at Re=5772 for the axial wave-number 1.02 (Orszag, 1971). Moderately careful experiments in pipe flow (Hagen-Poiseuille) demonstrate a transitional Reynolds number of the order 2000-3000. Most experimental observations in this area are related to slug or puff structures, which arrive with increasing frequency as the Reynolds number is monotonically increased (at a constant perturbation energy level). Similarly, piston-driven experiments for oscillatory flows in pipes have revealed a number of transitional stages, each characterised by macro-scale fluid properties. Turbulence associated with these periodic flows comes in bursts – often in the deceleration, or reverse-flow component of the cycle – is linked to the governing Reynolds number.

The initial numerical understanding for periodic pipe flow was laid-down by Yang and Yih (1977). Addressing the axisymmetric stability problem (2D) it was found that the flow tended towards neutral stability in the asymptote of Reynolds number, and monotonically so for increasing frequency. Later axisymmetric work by Fedele *et. al.* (2004) using long-wave Orr-Sommerfeld bases confirmed the known linear stability of periodic pipe flow.

In 2009 Nebauer and Blackburn (NB09) revisited the problem to extend the linear result to non-axisymmetric (3D) solutions. It was found that an increase in the three-dimensionality (in the azimuthal direction) for all Reynolds numbers studied resulted in an increase in the flow stability. The solution space extended that of Yang and Yih in both Reynolds number and frequency parameter. This extension confirmed the prediction of Yang and Yih that the flow is asymptotically stable to all perturbations.

The stability of oscillatory pipe flow is closely related to the stability of oscillatory Stokes layers, and of oscillatory channel flow. Instabilities in these flows were recorded by Blennerhasset and Bassom (2002 and 2006); in the latter, axisymmetric instability of oscillatory pipe flow was also reported. Further, Thomas *et. al.* (2012) recently reported non-axisymmetric instabilities of oscillatory pipe flow. These findings have prompted us to implement a different numerical approach to the study of instability in

oscillatory pipe flow than was previously used in NB09. The present work focuses on the development and validation of a fully spectral (Chebyshev–Fourier–Fourier) LNS solver and its use in studying Floquet instability of oscillatory pipe flow using time-stepper type methods (Tuckerman and Barkley, 2000). The solver is based on the work of Meseguer and Trefethen (2001) and uses a set of divergence-free (DF) basis as the trial functions in a spectral solution. The time-stepper LNS solver is coupled to a Krylov-Arnoldi iterative method for Floquet stability analysis.

PROBLEM GEOMETRY AND PARAMETERS

We start with a regular, rigid cylinder of radius R (diameter D) and length l. It is completely filled with a laminar, viscid and incompressible fluid of density ρ and viscosity ν. The governing equation for this system is the Navier-Stokes partial differential system;

$$\partial_t \mathbf{u} = -\mathbf{u}\cdot\nabla\mathbf{u} - \nabla p + \nu\nabla^2\mathbf{u} \;\;,\;\; \nabla\cdot\mathbf{u} = 0. \qquad (1)$$

Here p is the kinematic or modified pressure and $\mathbf{u}=\{u,v,w\}$, the primitive velocities in the radial, azimuthal and axial (r,θ,z) directions.

Under a constant pressure gradient and application of the no-slip wall boundary condition, the system (1) has an analytical solution:

$$u(r) = \frac{\Pi_0}{4\rho\nu}\left[1-\left(\frac{r}{R}\right)^2\right] \quad \forall\theta, z \quad \partial_r p = 0. \qquad (2)$$

The pressure gradient Π_0 is real and ∂_r represents the partial derivative with respect to r.

A closed-form solution of (1) for time-periodic pipe flows, under a periodic pressure gradient, can be obtained as analytical Bessel–Fourier solutions, first published by Sexl (1930) and later by Womersley (1955):

$$u_n(r,t) = \Re\left[\frac{K_n iT}{\rho 2\pi n}\left(\frac{J_0\left(i^{3/2}Wo2\frac{r}{D}\right)}{J_0\left(i^{3/2}Wo\right)}-1\right)e^{2\pi i n t/T}\right] \qquad (3)$$

where

$$Wo = R\,(\omega/\nu)^{1/2} \qquad (4)$$

is a dimensionless frequency parameter known as the Womersley number, n is a frequency harmonic, J_0 is the zeroth-order complex Bessel function, K_n is an associated complex axial pressure gradient amplitude, and T is the period of the oscillation. In the limit as T grows without bound, this analytical solution asymptotes to the standard parabolic Hagen-Poiseuille solution for the steady laminar flow in a circular pipe, *i.e.* (2).

The Reynolds number of the flow is based on the peak area-average velocity (see Nebauer and Blackburn 2009) and the pipe diameter;

$$Re = u_p \mathrm{D}/\nu \qquad (5)$$

Alternative formulations of type (3) are available for differing physical investigations. Harmonic piston or wall-driven systems vary slightly in their amplitude terms, or by the subtraction term (in the case of wall-driven flow). However, the underlying structure is a Bessel function quotient of a non-dimensional frequency. Blennerhassett and Bassom (2006) demonstrated that such scaling is immaterial in the linear dynamics – save only in the non-dimensional representation of the results.

The stability analysis problem is also solved in primitive variables. Starting from (1) it is proposed that $\mathbf{u} = \mathrm{U} + \mathbf{u}'$, where U is the base flow whos stability is examined and $\mathbf{u}'$ is an infinitesimal perturbation, of the form

$$\mathbf{u}'(r,\theta,z) = e^{i[\alpha z+\beta\theta]}\,\mathbf{u}'(r), \qquad (6)$$

where α and β are wave numbers in the axial and azimuthal coordinates respectively. Upon substitution and retaining terms linear in $\mathbf{u}'$, the linearized Navier-Stokes equations are obtained:

$$\partial_t\mathbf{u}' = -\mathbf{u}'\cdot\nabla U - U\cdot\nabla\mathbf{u}' - \nabla p' + \nu\nabla^2\mathbf{u}' \;,\quad \nabla\cdot\mathbf{u}'=0. \qquad (7)$$

All base flows considered in this study are axisymmetric and invariant along the axis of the pipe. Hence, $\mathrm{U}=\{u,v,w\}$ with $u=u(r)$, $v=0$ and $w=0$. Furthermore, we note that in the present problem, the base flow is T-periodic, *i.e.* $\mathrm{U}(t+T)=\mathrm{U}(t)$.

As in all incompressible flows the pressure is not an independent variable, and as all terms are linear in $\mathbf{u}'$, we can write this evolution equation in symbolic form (discarding the prime (') for convenience);

$$\partial_t\mathbf{u} = L(t)\mathbf{u}, \qquad (8)$$

where L is a linear operator with T-periodic coefficients through the influence of the base flow.

Correspondingly the stability of (8) is a linear temporal Floquet problem (Ioose and Joseph, 1990). Writing the state evolution of $\mathbf{u}$ over one period as

$$\mathbf{u}(t+T) = \boldsymbol{A}(T)\mathbf{u}(t), \qquad (9)$$

where $\boldsymbol{A}(T)$ is the system monodromy, or state-transition operator, we obtain a Floquet eigenproblem:

$$\boldsymbol{A}(T)\mathrm{u}''_j(t) = \mu_j \mathrm{u}''_j(t). \qquad (10)$$

Here $\mathrm{u}''_j(t)$ are phase-specific Floquet modes and μ_j are Floquet multipliers. Stability of the problem is assessed from the Floquet multipliers: unstable modes have multipliers that lie outside the unit circle in the complex plane (i.e. $|\mu|>1$), while stable modes lie inside (i.e. $|\mu|<1$).

A key point about the approach is that a system monodromy matrix $\boldsymbol{A}(T)$ is not explicitly constructed. Rather, a Krylov method is used that is based on repeated application of the state transition operator whose action is obtained by integrating the LNS equations forward in time over interval T.

NUMERICAL METHODS

Three methodologies are handled here; a spectral-element method cast in either Cartesian or cylindrical coordinates, and a divergence-free spectral method formulated in Chebyshev polynomials for the non-spectral directions.

Spectral-Element Formulation (SE)

We use a time-stepping based methodology given detailed explanation in Barkley *et. al.* (2008), and previously used

in studies of various oscillatory flows (e.g. Blackburn 2002 and Blackburn and Sherwin, 2007) in order to solve the Floquet eigenproblem. The time-periodic base flows are precomputed at a moderate number of phase points or time-slices and then may be accurately reconstructed during timestepping via a Fourier interpolation in time.

Cylindrical Coordinates

Spatial discretization and time integration for both the LNS and DNS problems is handled using a cylindrical coordinate spectral element method with mixed explicit/implicit time stepping, as outlined in Blackburn and Sherwin (2004). The domain is discretized into spectral elements in the meridional semi-plane that runs from the pipe axis to the outer radius in the radial direction and a finite length of pipe l_z in the axial direction, as shown for example in figure 1.

Fourier modal structure is assumed in the orthogonal cylindrical direction. The solution set is restricted to integer wavenumbers β, being 0 for axisymmetric cases. In the axial direction we use real wavenumbers [illegible] D/l. Because of the approach taken to spatial discretization in the axial direction, the Floquet eigensolution for any domain length can contain modes for both [illegible] (i.e. modes that are axially invariant) and [illegible] m [illegible] D/l_z (where m is an integer).

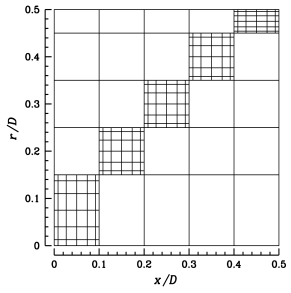

Figure 1: 2D planar mesh for cylindrical geometry.

Cartesian Coordinates

An alternate approach – and an internal consistency check on the cylindrical coordinate formulation – is to retain a Cartesian coordinate space for the 2D spectral-element mesh and allow Fourier modal structure in the pipe-axis direction. A circular element mesh (as in figure 2) is used with no-slip boundary conditions at the wall. The nature of Fourier solutions in the axial direction implicitly applies periodic flow conditions to the cylinder end-caps.

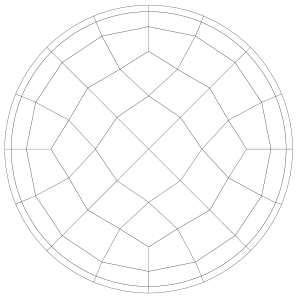

Figure 2: Spectral elements of the Cartesian mesh. This discretization allows control of the axial wave number, but limited influence on the azimuthal wave number.

As in the cylindrical coordinate space, the use of a 2D element mesh reduces control over the spectral symmetry mode number associated with that plane. For the Cartesian space, we compute sufficient leading modes to identify $\beta>0$ cases, which are typically sub-dominant.

Spectral Divergence-Free Formulation (DF)

An alternate to, and in the imposition of $\nabla\cdot\mathbf{u}=0$ – as a separate Poission solution step – is the use of divergence-free basis functions. The numerical method we are using in this case is based on the work of Meseguer and Trefethen (2003). The original divergence free basis methodology is developed in detail by Leonard and Wray (1982).

The underlying principle in this solution space is the implicit assertion that the three-dimensional flow can be constructed from two velocity components, given that the divergence of that field is confined to zero. Hence, $\mathbf{v}=\{v_1, v_2\}$, from which a full third component may be calculated.

To develop this concept we note that the operator system (8) can be projected by the inner product of the operator over a suitable space,

$$<\partial_t\mathbf{v}, W> = <L\mathbf{v}, W>, \quad \forall W; \tag{11}$$

here $<\cdot, \cdot>$ defines the inner product over the spatial domain. In the construction of W we note that $\mathbf{v}$ is solenoidal (*i.e.* divergence free) and the test space W should conform for favourable properties. This is of particular interest since $<v_1,W> = <v_2,W>$ for all solenoidal functions W that vanish over the boundary.

From (1) the pressure is imposed by ∇p, which upon projection in W presents as $<\nabla p, W>$. Integration by parts of this expression yields

$$<\nabla p, W> = pW - <p,\nabla W>. \tag{12}$$

The product pW of (12) is zero provided W=0 at the boundary. Further more, $<p,\nabla W> = 0$ as $\nabla\cdot W$=0. Hence, the pressure has been removed as a variable from the system. In addition the Poisson solution ($\nabla\cdot\mathbf{u} = 0$) step has been removed due to the inherent divergence-free nature of the basis space W.

In constructing L we start by defining the matrix evolution problem in dual and solenoidal vector space,

$$B\mathbf{u}_t = A\mathbf{u}, \quad B=<W,\mathbf{v}>, \quad A=<W,L\mathbf{v}> \tag{13}$$

hence, $L=B^{-1}A\mathbf{u}$. Subsequently, the classical solution to a time-invariant base-flow (such as that of Hagen-Poiseuille flow) is interchangeable with

$$e^{Lt}\mathbf{u} \leftrightarrow \int_0^T L\mathbf{u}dt. \tag{14}$$

With this operator notation, it is possible to compare our time-stepper approach (with a time-invariant base flow) with a direct eigenvalue decomposition. To perform the temporal integration we use a semi-implicit 2nd order stiff solver, stemming from the numerical differentiation formulas as implemented in Matlab's `ode15s`. The Hagen-Poiseuille (HP) stability problem is solved using

60 Chebyshev radial nodes. Comparison over the leading values of the spectrum shows very good alignment, as in figure 3.

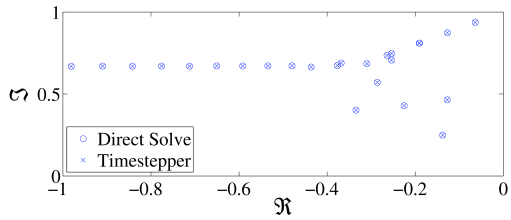

Figure 3: Comparative study of the HP spectrum for Re = 2000, α=1 and β=0 through direct decomposition of the time-invariant operator (○) and through temporal integration of (13) marked as (×).

Schmid and Henningson (2000) provide tabulated eigenvalues for HP flow at Re=2000, α=1 and β=0. The leading three eigenvalues, as calculated by the two DF formulations are compared in table 1.

#	Schmid and Henningon	Direct Solve (14)	Time-Stepper (14)
1	-0.0637455	-0.0637455	-0.063741**7**
2	-0.0637455	-0.0637455	-0.063742**2**
3	-0.1269911	-0.1269911	-0.126990**2**

Table 1: Leading three eigenvalues (real-part only) of HP flow: Re = 2000, α=1, β=0 (axisymmetric). Each form of (14) is computed. While eigenvalues 1 and 2 are the same to printed precision, they do differ, and are not complex-conjugate modes.

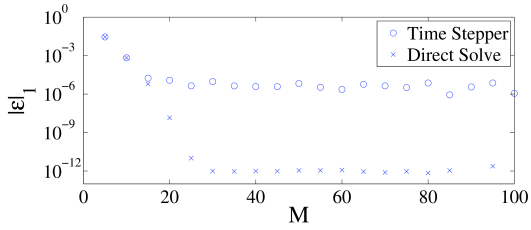

Figure 4: The absolute difference (|ϵ|) between the computed eigenvalue for M modes and 100 modes of the direct solution, as in table 1. Spectral convergence is observed for both solution types. The 'wiggle' in the high modal values is due to the increase in the matrix condition number (κ).

The spectral convergence of the timestepper methodology is demonstrated in figure 4. The plateau at 10^{-5} is related to the repeated application of the high condition-number operator matrix, a product of the inversion of B. Special care is taken by Meseguer and Trefethen to energy-weight and condition the resulting operator. The same technique is not possible for the timestepper approach.

The Time-Dependent Operator

By replacing the base-flow definition of L with one which is time-periodic, the only term of (7) affected is the linear advection—diffusion term. Hence the system's time dependence is limited to the advancing inner-products,

$$<\mathbf{v}_\tau, W> = <L(t)\,\mathbf{v}_0\,, W>, \qquad (15)$$

for any initial solenoidal state $\mathbf{v}_0$ and final state $\mathbf{v}_\tau$. The weak-form of (7) can then be expressed as an integral over a period, T:

$$\mathbf{u}_T = \int B^{-1}\left[W\left(\nabla^2 + \nabla \mathrm{U}(t)\cdot\mathbf{u}(t) + \mathrm{U}(t)\cdot\nabla\mathbf{u}(t)\right)\right]\mathbf{u}(t)\;dt. \qquad (16)$$

Therefore, the complexity of constructing the operator matrix is linked to the inversion of B. In (16) the operator matrices B, W and ∇^2 are constant. Hence, the preconditioning of B^{-1} is constructed only once.

Comparison of the DF and SE methodologies

We test the implementation of (16) using the base-flows constructed for NB09, as defined in (3), against the previously published SE results.

Cylindrical Coordinates

For the least stable case of NB09 (α=0,β=0) we find an exact alignment of the two solution methodologies to numerical precision, see figure 5. These results are identical to 5 decimal places. From (6), the role of spatial wave numbers for this case is eliminated, and the perturbation is confined to the structure in $\mathbf{u}(r)$. The excellent agreement of this data points towards the successful implementation of centre-line basis and Fourier conditions.

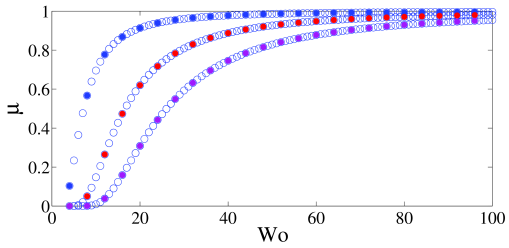

Figure 5: Axially invariant, axisymmetric (α=0, β=0) Floquet Multipliers for both the SE(○) and DF(●) formulations, showing the first 3 modes respectively.

Utilising the azimuthal control this SE space has, we test the DF algorithm for three-dimensional wave numbers, in the axially-invariant domain. Figure 6 demonstrates the alignment of the two solution methodologies, and simultaneously the effect of an adaptive-step temporal resolution in the DF method. While the alignment is very good for higher Wo, the lower Wo can suffer as integration times can be large for moderately low Re. The adaptive-step, stiff solver used in the DF is better equipped to navigate around quickly changing state space.

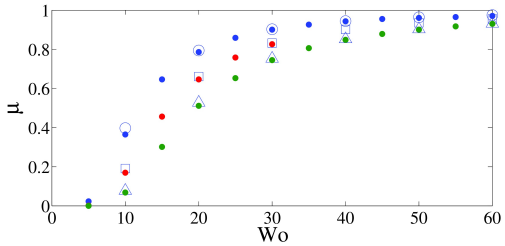

Figure 6: Axially invariant, non-axisymmetric (α=0, β>0) Floquet Multipliers for both the SE(●) and DF methods delineated by β=1 (○), β=2 (Δ) and β=3 (□) and showing the first mode only for each azimuthal wave number.

The sub-dominant modes associated with α>0 are compared in figure 7 with the cylindrical coordinate SE

method. Again, the difficulties in resolving low Wo flows in fixed-step integration are highlighted. As these modes are sub-dominant to most axially in-variant cases, a much deeper eigenvalue search from the Arnoldi solver was required.

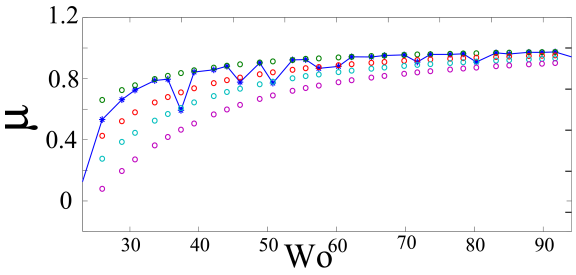

Figure 7: Axially variant, axisymmetric ($\alpha > 0$, $\beta = 0$) Floquet Multipliers for both the SE($*$) and DF(o) formulations.

The combined effect of sub-dominance and wave-number control in the SE method for this parameter space makes the alignment for α>0 difficult to observe. However the level-locking of μ over Wo is observed (the SE method finds 'a' result in the eigenvalue stack, not necessarily the leading one for all cases), and we expect better alignment as integration time-step in the SE method is tightened, currently at $\Delta t = 10^{-3}$. The performance of the DF formulation is evident, and is an order of magnitude cheaper to compute than the SE equivalent.

Cartesian Coordinates

An available internal consistency check, and better validation point for the DF over axial wave-numbers is the Cartesian Fourier modal methodology. Figure 8 presents the SE results (plotted as o) along with the DF (+ and x). Very good alignment of the points is observed, with the general trends of the two methodologies in agreement. The SE method (having converged an eigenvalue 'stack' for a given axial wave number) is plotted as one marker-type due to the minimal level of control over azimuthal wave number. An apparent result, yet to be tested as a valid Floquet mode, is found as $\alpha = 0 \rightarrow 0^{+}$.

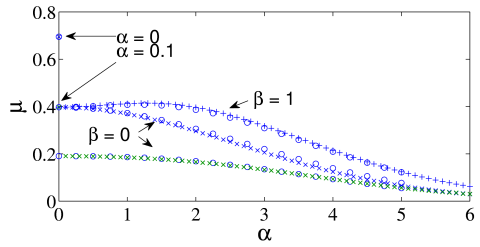

Figure 8: Influence of the axial wave number for Wo =10, Re = 400/(2π). Cartesian SE(o) results differ slightly from the DF (β=1; +, and β=0; x) for the dominant solutions, though offer very good agreement for α=0 and as α is increased.

Floquet Mode at α=0

There is a clear distinction between the leading Floquet multiplier for the axially-invariant cases, and the rest of the axial spectrum. To demonstrate this, a log-scale of axial wave-number is used in Figure 9. The continuation of the spectrum is observed over α to 10^{-5}, which then terminates with an abrupt jump at α=0.

As $\alpha \rightarrow 0$ the wave length of the disturbance grows without bound. This is analogous with that of the base-flow's period asymptote to HP flow. This jump in the Floquet multiplier was found to be synonymous with viscid, axisymmetric HP flow.

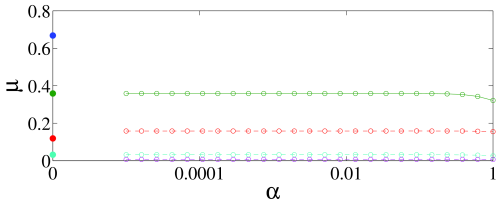

Figure 9: The log-linear plot of axisymmetric eigenvalues for Re=2000, Wo=30 for α=0 (●) and α>0 (○). A clear continuation as $\alpha \rightarrow 0$ of the dominant modes is observed, with the apparent mode much removed from the rest.

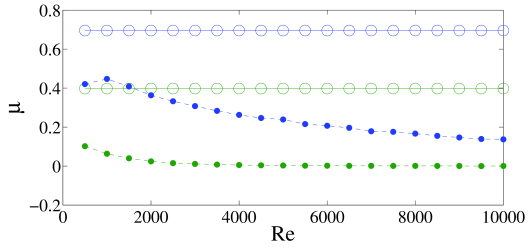

Figure 10: Floquet multipliers (leading two) of the apparent mode (○) for Wo=10, plotted over Re. A spiral mode, α=1, β=1 (●) is viscid, as are all axially-variant, or three-dimensional (β>0) modes.

This apparent discontinuity is confined to axisymmetric cases, and then only at axially-invariant wave-number 0. This mode is inviscid, being independent of Re (see figure 10), however it is viscous-temporally dependent, demonstrated by viscosity appearing in the Womersley number. The mode is characterised by axial-velocity structure, as determined by NB09. The axially-variant mode for α=0.1 is clearly very different, a high swirl mode, with little axial-velocity component (figure 11).

The presence of the apparent mode in all three of the calculation methodologies (based on two separate solution procedures) is one indication that the Fourier parity conditions at the pipe centre-line have been implemented correctly in the DF formulation.

Spurious modes are known to exist in many eigenvalue studies, including Floquet related cases, where the meta field is (or near) autonomous (see Elston *et. al.* 2004). A physical example is the spring-mass system, which has a leading autonomous Floquet multiplier of 1.

The oscillatory pipe flow is analogous to a sping-mass-damper system, which offers a physical explanation of a damped autonomous mode. An alternate physical reasoning occurs in the limit of pipe-length (α=0). Here, swirl modes switch off and give way to axial-modes, giving rise to a discontinuity when there is no mechanism available over a period to misalign the linear operator's eigenspace with the fluid.

Such near-wall and centre-line structure of the eigennmodes can be found in modes which are considerably sub-dominant. One example is the 4th mode of α=1, β=3 for Wo=10, which is the subject of a DNS study, and lies outside the scope of this paper. The mode's iso-contours of axial velocity component (+ out of page, -

into) is shown in figure 12. A case for large transient-growth of these decaying modes, with clear inflection and wall structures, can be made, and is again, a topic outside the scope of this paper.

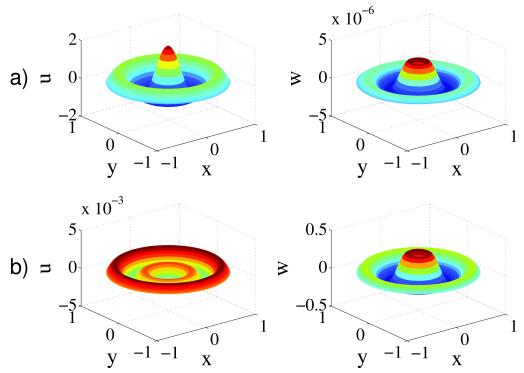

Figure 11: Surface plots of the leading (least-stable) Floquet Modes for Wo=10, Re=1000, β=0, α=0 (**a**) and α=0.1 (**b**), as projected into axial (**u**) and azimuthal (**w**) velocity components. Here, a swirl-mode (**b**) is reduced to a non-swirl mode (**a**), both of which have little or no radial component.

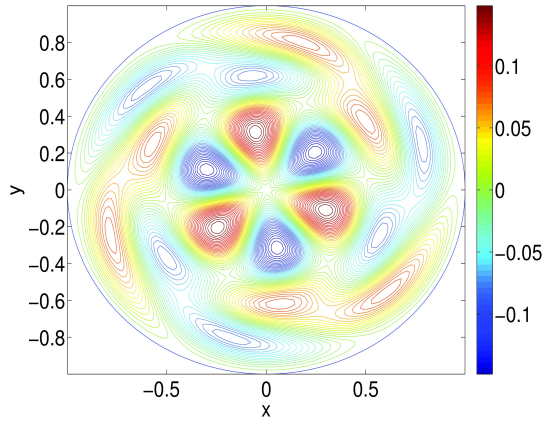

Figure 12: The 3rd sub-dominent (4th mode) eigenvector of Wo=10 , Re=1000 for $\beta = 3, \alpha = 1$.

CONCLUSION

A spectral collocation method has been modified to compute the Floquet stability of time-periodic pipe flow. The key advantage of the new methodology lies in the divergence-free basis functions used. Through application of the solenoidal space the unique mathematical conditions are provided for the elimination of the pressure state space. Not only is the variable removed from the system, but the requirement to entertain a Poisson sub-step is also avoided.

The methodology has been tested against known time-invariant, and periodic stability cases and found to agree favourably. The flexibility of the new method is also evident in complete control over the spatial wave numbers.

Using this high fidelity solver we are now proceeding to provide a comprehensive check of linear instabilities previously reported in the literature.

REFERENCES

BLACKBURN, H. (2002) "Three-dimensional instability and state selection in an oscillatory axisymmetric swirling flow", Physics of Fluids, **14**, 3983

BLACKBURN, H. and SHERWIN, S. (2004) "Formulation of a Galerkin spectral element--Fourier method for three-dimensional incompressible flows in cylindrical geometries", J. Computational Physics, **197**(2), 759—778

BLACKBURN, H. M. and SHERWIN, S. J. (2007), "Instability modes and transition of pulsatile stenotic flow: pulse-period dependence." J. Fluid Mech, **573**, 57–88.

BARKLEY, C. BLACKBURN, H. (2008), "Convective instability and transient growth in flow over a backward-facing step", J. Fluid Mech., **603**(1), 271—304.

BLENNERHASSETT, P.J. and BASSOM, A.P. (2002) "The linear stability of flat Stokes layers" J. Fluid Mech., **464**(1), 393—410

BLENNERHASSETT, P.J. and BASSOM, A.P. (2006), "The linear stability of high-frequency oscillatory flow in a channel", J. Fluid Mech.,**556**(1),1—25

ELSTON, J. R., SHERIDAN, J. and BLACKBURN, H. M. (2004), "Two-dimentional Floquet stability analysis of the flow produced by an oscillating circular cylinder in quiescent fluid", Euro. J. Mech. B – Fluids. **23**, 99-106.

ENEZ, J.J.I.M and PINELLI, A. (1999), "The autonomous cycle of near-wall turbulence", J. Fluid Mech, **389**,335-359

FEDELE, F., HITT, D. and PRABHU, R. (2004), "Revisiting the Stability of Pulsatile Pipe Flow", Euro. J. Mech. B – Fluids. **24**, 237-254

IOOSS, G. and JOSEPH, D. (1990), "Elementary Stability and Bifurcation Theory", 2nd edn. New York: Springer.

LEONARD, A. and WRAY, A. (1982), "A new numerical method for the simulation of three-dimensional flow in a pipe", *In Proc.* Eighth International Conference on Numerical Methods in Fluid Dynamics, 335—342.

MESEGUER, A. and TREFETHEN, L.N, (2003), "Linearized pipe flow to Reynolds number 10^7", Journal of Computational Physics, **186(1),** 178—197.

NEBAUER, J. and BLACKBURN, H. (2009), "Stability of Oscillatory and Pulsatile Pipe Flow", CSIRO:CFD7, Melbourne, Australia.

ORSZAG, S.A, (1971), "Accurate solution of the Orr-Sommerfeld stability equation", J. Fluid Mech, **50**(4), 689-703

SCHMID, P. and HENNINGSON, D. (2000), "Stability and Transition in Shear Flows", Springer. V142 Applied Mathematical Sciences, MARSDEN, J. and SIROVICH, L.

SEXL (1930), Z. Phys. **61,** 349

THOMAS, C., BLENNERHASSETT, P.J. and BASSOM, A.P. (2012) "The linear stability of oscillating pipe flow", Physics of Fluids, **24**(1), 014106—014106

TUCKERMAN L.S, and BARKLEY, D. (2000), "Bifurcation analysis for timesteppers", IMA Volumes in Mathematics and its Applications, **119,** 453—466.

WOMERSLEY, J. R. (1955) "Method for the calculation of velocity, rate of flow and viscous drag in arteries when the pressure gradient is known.", J. Physiology **127**, 553–563.

YANG, W. H., & YIH, C. S. (1977). Stability of time-periodic flows in a circular pipe. *J. of Fluid Mech.*, ***82***, 497-505.